

## Toxicity of Zinc Oxide Nanoparticles Prepared with Plasma Jet for in Vitro and in Vivo Study

Ban H. Adil,<sup>1\*</sup> Waseem K. Kaith,<sup>2</sup> Souad G. Khalil<sup>1</sup> and A.S. Obaid<sup>3</sup>

<sup>1</sup>Department of Physics, College of Science for Women,  
University of Baghdad, Baghdad, Iraq

<sup>2</sup>Ministry of Health, Al-Yarmouk Hospital, Baghdad, Iraq

<sup>3</sup>Department of Physics, College of Science, University of Anbar, Ramadi, Iraq

\*Corresponding author: banha\_phys@csw.uobaghdad.edu.iq

Published online: 18 June 2024

To cite this article: Adil, B. H., Kaith, W. K., Khalil, S. G. & Obaid, A. S. (2024). Toxicity of zinc oxide nanoparticles prepared with plasma jet for in vitro and in vivo study. *J. Phys. Sci.*, 35(1), 53–65. <https://doi.org/10.21315/jps2024.35.1.5>

To link to this article: <https://doi.org/10.21315/jps2024.35.1.5>

**ABSTRACT:** *This study shows how zinc oxide nanoparticles (ZnO NPs) affect the blood component of adult male rats utilising a safe, simple and inexpensive plasma jet production approach for varying exposure periods. The ZnO NPs were described as follows: the X-ray diffraction (XRD) pattern showed that in the UV-visible spectrum of the peak region at 291 nm to 302 nm, the strong intensity peaks indicated the crystalline nature of the ZnO NPs. A field emission scanning electron microscopy (FE-SEM) was used to look at the morphology of the ZnO NPs. The diameters of the spherical particles ranged from 30 nm to 96 nm. Two sets of ZnO NP dosages are used to investigate the impact of ZnO NPs on component blood. White blood cells (WBC), red blood cells (RBC), haemoglobin (HB) and platelets (Plt) components in the blood increase when ZnO NPs dosages rise. The cytotoxicity of the rat embryonic fibroblast (REF) normal cell line is calculated concurrently and the highest cytotoxicity equals 9% at 100% ZnO NPs concentration. These results suggest that a variety of blood component-affecting disorders may be treated using the ZnO NPs receptor.*

**Keywords:** ZnO NPs, cold plasma, cytotoxicity, liver function, kidney function

### 1. INTRODUCTION

Nanotechnology is the science of altering systems at the atomic or molecular level to perform a variety of tasks, from the commonplace of making synthetic goods and vinyl and polymers better to the more exotic of making biological probes,

sensors and drug delivery systems.<sup>1</sup> Nanotechnology is a field of current research because of its unique properties and potential uses, which have long piqued the curiosity of scientists worldwide. They are quite groundbreaking in several areas, such as antimicrobials and nanomedicine. The development of biosensors has discovered intriguing applications for these marvels of technology. In addition to having a high specific surface area, nanomaterials also have a high surface area to volume ratio, which rises with decreasing particle size, dispersion and shape. Furthermore, the enhanced physical characteristics of the nanoparticles raise their reactivity.<sup>2</sup> The recently emerged topic of creating unique metal nanoparticles has generated a lot of attention in science. Numerous methods, including the sol-gel method,<sup>3</sup> chemical method,<sup>1</sup> green method,<sup>4</sup> pulsed laser deposition<sup>5</sup> and chemical precipitation method, have been suggested for the manufacture of these materials.<sup>6</sup> Zinc oxide nanoparticles (ZnO NPs) are one such inorganic metal that may be used as a medication, an antibacterial agent, or a package preservative. It easily permeates food goods, eliminates microbes and protects humans from disease.<sup>7</sup> ZnO NPs have been successfully tested in vitro as an antibacterial agent against *Salmonella typhi* and *S. aureus*.<sup>8</sup> ZnO is used in transparent electronics, ultraviolet light sensors,<sup>9</sup> piezoelectric devices, chemical sensors and spintronics (ZnO doped with magnetic transition metals) because of its special qualities and wide range of applications such as, nanomaterials.<sup>10,11</sup> Several morphologies of these nanostructures have been created, including nanoflakes, nanorods, nanobelts, nanorings, nanocables, nanotubes, nanocolumns, nanocombs and nanoneedles.<sup>12</sup> The tiny particle size of nano-ZnO makes zinc easier for the body to absorb. As a result, food additives with nano-ZnO are widely used. The US Food and Drug Administration (FDA) also lists ZnO as a medication that is generally recognised as safe (GRAS).<sup>13</sup> Because ZnO nanoparticles have so many medicinal uses, increasing interest has been shown in their prospective biomedical uses. In terms of biological uses, ZnO NPs are less expensive and less dangerous than other metal oxide nanoparticles. Among these applications include anticancer, medication delivery, antibacterial, diabetic care, anti-inflammation, wound healing and bioimaging.<sup>14,15</sup> This search aims to synthesise zinc nanoparticles (Zn NPs) using a plasma jet and investigate the effects of component blood, kidney, liver and cytotoxicity of rat embryonic fibroblast (REF) cells line.

## 2. MATERIAL AND METHOD

### 2.1 Synthesis of ZnO NPs

ZnO NPs were synthesised by nonthermal plasma using argon (Ar) gas. The cold plasma system consisted of a gas flowmeter with a calibrator of 1 min/L–2 min/L. They can withstand DC voltages of up to 25 kV and are linked to the cathode of

the power supply. A small flask (25 mm in size) is filled with the glass beaker holding the deionised water, and the flask is placed under the metal tube on a moving holder. The anode was a Zn plate with flat ends that was 25 cm in length and 10 cm in width. It had a purity rating of 99%. The volts' anode (anode) is equipped, and the beaker was placed under the metal tube to the distance between the water surface, for different exposure times of plasma (6, 8 and 10) min. Gas in the metal tube was regulated by the flowmeter to control the gas flow of 3 min/L. Plasma was generated between the tube and the surface of the water as shown in Figure 1.<sup>16</sup>



Figure 1: Synthesis of ZnO NPs by plasma jet.

## 2.2 Cytotoxicity of ZnO NPs in Vivo Study

### 2.2.1 Animals

Eighteen adult male rats, weighing between 150 g and 200 g, were housed in plastic cages in a temperature-controlled environment that was regulated between 20°C and 25°C. They were fed and hydrated daily. The study uses 18 adult male rats, divided into three groups of six rats each, and gave two of the groups into two dosages (0.5 and 1) ml. The control group was the third group. Then, the weight of each rat was recorded daily, starting from the day before dosage, which marked the first day of the trial. This allowed scientists to use equation (1) to determine each group's proportional importance.<sup>14</sup> Red blood cells (RBC), white blood cell (WBC), hemoglobin (HB) and platelets (Plt) percentages are also assessed for each group and each rat before to treatment. Every two weeks, the dosage was repeated, with a 48 h gap between each administration. After the dosage cycle,

all rats (of all groups) had their blood extracted right away. Combined blood was then utilised to determine the rate of rise or reduction over a six-week period. Sixteen rats from all groups had their blood collected, and during the research period, the levels of liver and renal enzymes were monitored and contrasted with those of the control group.

$$RRW = \frac{W(di)}{W(d0)} \quad (1)$$

RRW represents the relative rate weight,  $W(di)$  is weight of rate during study time and  $W(d0)$  is weight of rate on the first day of the study.

### 2.3 Cytotoxicity of ZnO NPs in Vitro Study

The cytotoxicity experiment performed in this study was conducted using the rat embryonic fibroblast (REF) cell line. A microtiter plate containing 96 (128) flat wells and 10,000 normal cells per well was utilised for tissue cultivation. Turning the microtiter plate upside down demonstrates that it was incubated at 37°C for 24 h. ZnO NPs were added to cells at escalating concentrations (100%, 50%, 25%, 12.5% and 6.25%), while control wells were left undisturbed. The steps were performed in triplicate and at 37°C for a duration of 24 h. The solution obtained from the control group is the deepest violet in colour because 50 µl of solution was added, fixed and stained using a crystal violet assay in every well. To quantify the percentage of variability normal cells (toxicity rate), a microtiter plate reader was used to read the results at 492 nm wavelength. Equation (2) is then used to get the mean value for each group.<sup>17</sup> The mean value for every group will then be approximated. GraphPad Prism v7.0 was used to evaluate the experimental results where \* $P < 0.5$ , \*\* $P < 0.1$ , \*\*\* $P < 0.01$  and \*\*\*\* $P < 0.001$ .

$$GI\% = \frac{(Vc - Vt) \times 100\%}{Vc} \quad (2)$$

Where  $Vc$  represent control,  $Vt$  represents treated and  $GI$  is growth inhibition rate

## 3. RESULT AND DISCUSSION

### 3.1 UV-Visible Absorption Spectrum

A spectral analysis tool was used to demonstrate the formation of the NP at visible light wavelengths, and Figure 2 illustrates the exposure time function for the UV-visible absorption spectra of colloidal ZnO NPs. When ZnO NPs are exposed for 10 min as opposed to the other duration, there is an increase in absorbance in

the UV-visible spectrum, with the peak area expanding from 291 nm to 302 nm. The production of ZnO NPs is demonstrated by the strong peak at around 302 nm and increased intensity may be related to the growing amount of ZnO NPs created as a result of the reduction in Zn ions present in aqueous solutions.<sup>18</sup>

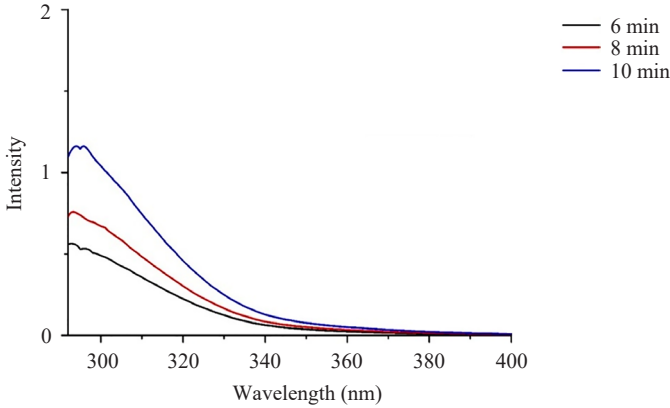


Figure 2: UV-visible spectrum of ZnO NPs as different of exposure time.

### 3.2 The Result of X-Ray Diffraction

The X-ray diffraction (XRD) pattern in Figure 3 shows the hexagonal wurtzite phase of the ZnO structure of ZnO nanoparticles. The material's crystalline nature is shown by the strong diffraction peaks that were seen. Three diffraction peaks,  $36.34^\circ$ ,  $39.06^\circ$  and  $43.28^\circ$  which correspond to (002), (100) and (101), occur in the diffraction pattern of the as-prepared Zn NPs after a 6 min exposure period. Four diffraction peaks appeared at diffraction angles  $36.34^\circ$ ,  $39.06^\circ$ ,  $43.28^\circ$  and  $54.36^\circ$  in the diffraction patterns of the samples generated with exposure times of 8 min and 10 min. These peaks correspond to (002), (100), (101) and (102) with a preferred orientation at (101). The crystallite was found as at an exposure time of 10 min, Zn NPs' HCP structure complies with the Joint Committee on Powder Diffraction Standards database (JPCDS card number: 36-1451). The Debye Sherrer formula, was used to determine the crystal size of ZnO NPS.<sup>19</sup>

$$D = \frac{k\lambda}{\beta \cos \theta} \quad (3)$$

Where D is the size of crystalline, k is a constant of 0.94,  $\lambda$  is wavelength of X-ray source,  $\beta$  is the full width at half maximum (FWHM) and  $\theta$  is the Bragg angle.<sup>20</sup> The average size of these ZnO NPs was roughly 70 nm, 50 nm and 55 nm for samples prepared at exposure time 6 min, 8 min and 10 min, respectively at prefer peak (101).

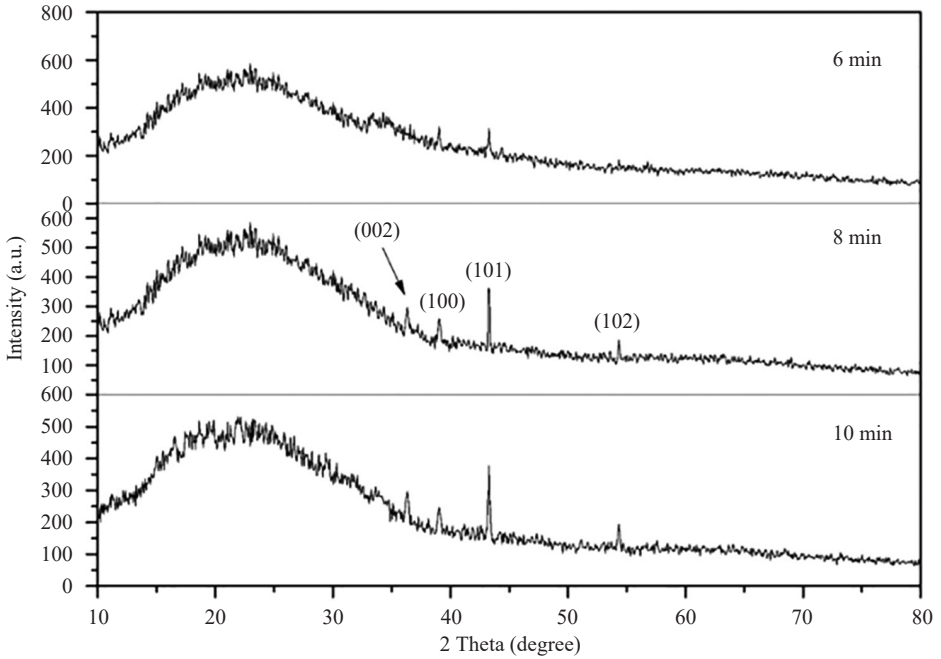


Figure 3: X-ray diffraction of ZnO NPs as different of exposure time.

### 3.3 Result of Field Emission Scanning Electron Microscopy (FE-SEM)

A morphological image of ZnO NPs prepared using cold plasma was shown in Figure 4. The image revealed that the ZnO NPs has spherical shape with the appearance of nanotubes that result from the aggregation of spherical particles, spherical particle of the information-goo nanoparticle size distributed in the range of 30 nm to 94 nm.

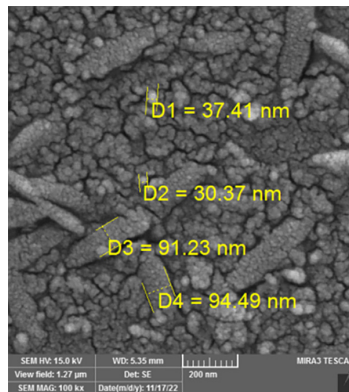


Figure 4: FE-SEM of ZnO NPs for 8 min exposure time.

### 3.4 Cytotoxicity Using the Normal Cells Line (REF)

Maximum cytotoxicity under a range of series-dilutions of ZnO NPs was attained in the scenario when 100% of the ZnO NPs exposure was at 9%, as in Figure 5.

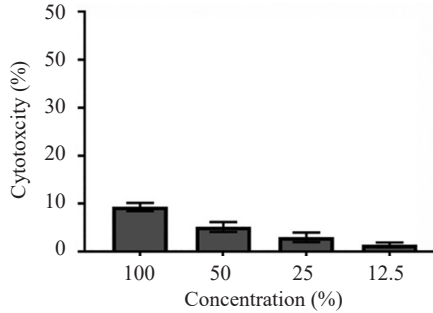


Figure 5: Testing the cytotoxicity of ZnO NPs on the REF cell line.

### 3.5 Effect ZnO NPs on Component Blood

The proportion of (WBC, RBC, HB and Plt) increase the study period of dose of Zn NPs exposure, as shown in Figures 6 to 9, the exposure length determined the difference between the component blood level on day 0 and day 50.

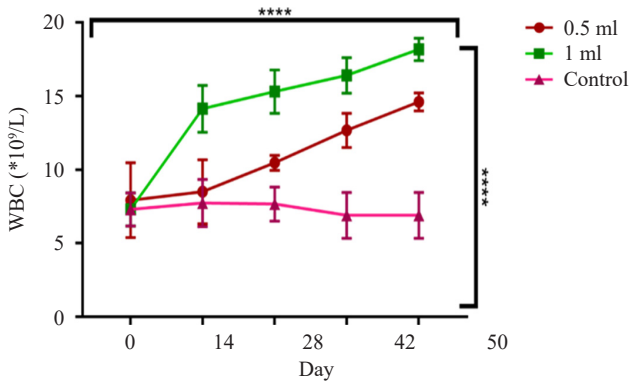


Figure 6: The WBC percentage in blood during 50 days.

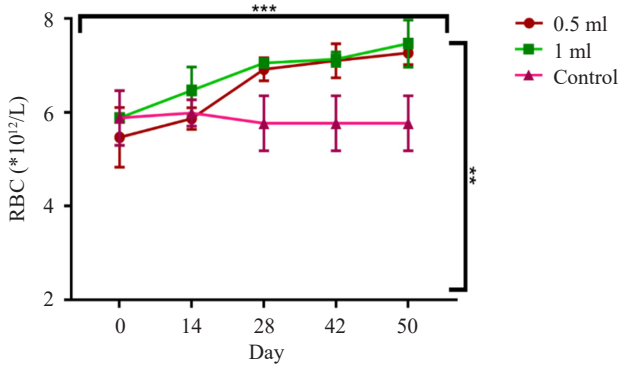


Figure 7: The RBC percentage in blood during 50 days.

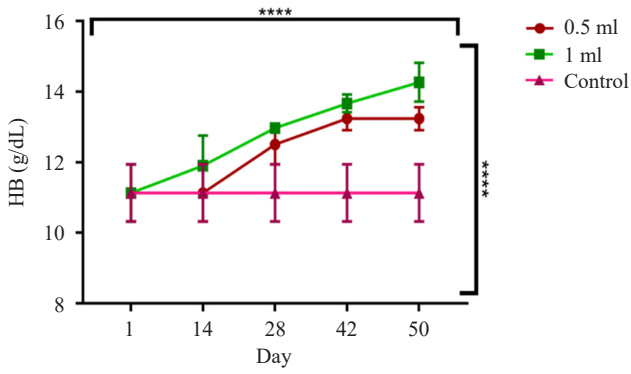


Figure 8: The HB percentage in blood during 50 days.

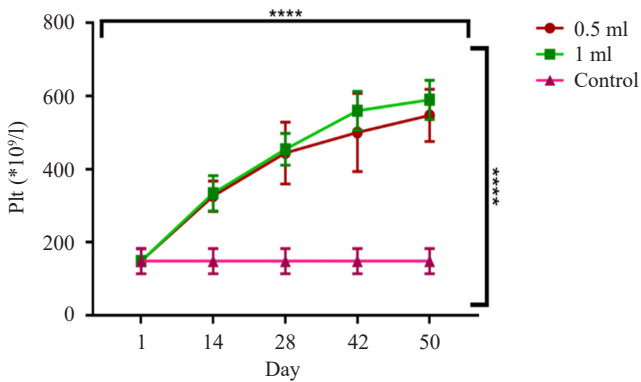


Figure 9: The Plt percentage in blood during 50 days.

### 3.6 Effect ZnO NPs on Liver Function

There is a significant increase of glutamic oxaloacetic transaminase (GOT) enzyme for the group that dosed 1 ml only, while glutamate-pyruvate transaminase (GPT) enzyme. There is a significant increase for the two groups that dosed 0.5 ml, 1 ml compared control group at  $p \leq 0.01$ ,  $p \leq 0.001$  receptivity, Figure 10 and Figure 11.

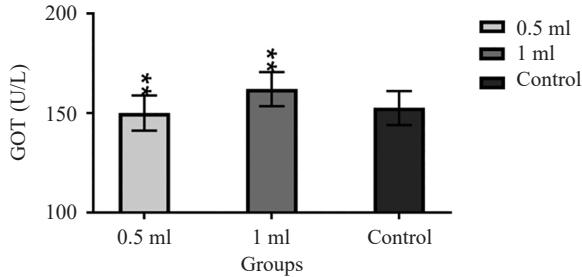


Figure 10: The liver function GOT level in rats' blood.

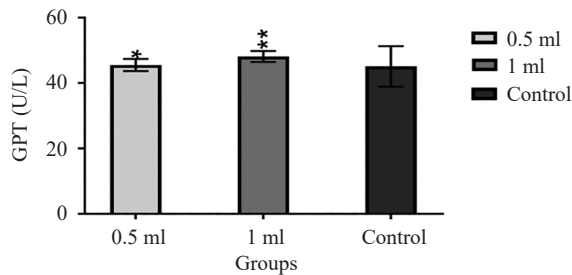


Figure 11: The liver function GPT level in rats' blood.

There is a significant increase in the ALP at (0.5 ml and 1 ml of ZnO NPs) for the period compared to the control group at  $p \leq 0.01$ ,  $p \leq 0.001$ , respectively, compared to the control group in Figure 12.

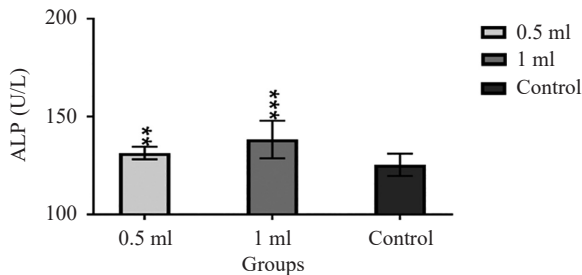


Figure 12: The liver function (ALP) level in rats' blood.

### 3.7 Effect ZnO NPs on Kidney Function

As for the level of kidney function in the forms represented by creatine, urea and uric acid, in Figure 13, Figure 14 and Figure 15, respectively, we note the preservation of their levels for both doses compared to the control group.

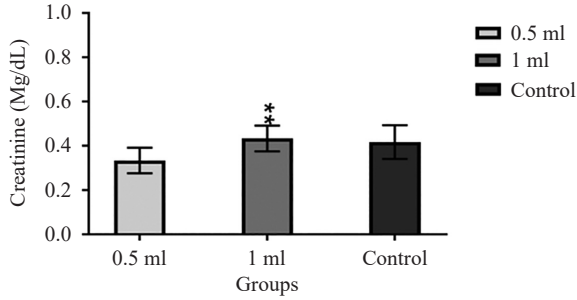


Figure 13: The kidney function (creatine) level in rats' blood.

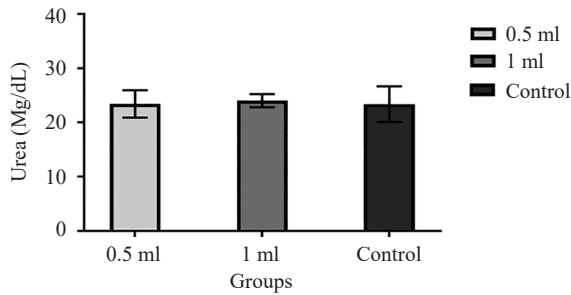


Figure 14: The kidney function (urea) level in rats' blood.

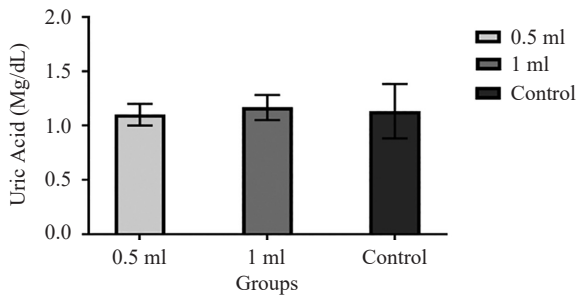


Figure 15: The kidney function (uric acid) level in rats' blood.

Figure 16 represent the relative weight rat during 50 days. A significant increase weight compares control group, which indicates the good of metabolic processes for all groups.

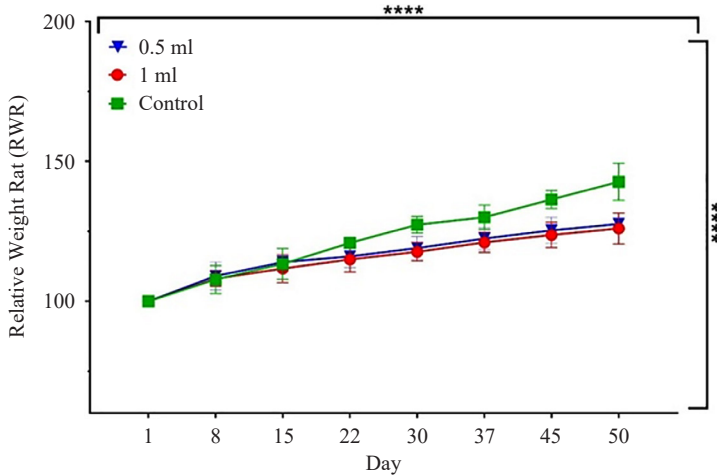


Figure 16: The relative weight rat during 50 days.

#### 4. CONCLUSION

Nanomaterials have a potential future for medical applications in general, especially nano-zinc. In this work, a simple methodology was employed to synthesise ZnO NPs by the plasma jet method. XRD examination indicated that each sample was polycrystalline. FE-SEM analysis of ZnO NPs shows that the particles were spherical in shape with the nanosize, as the results showed a positive effect on blood components, which in turn treats many blood diseases, as well as low cellular toxicity, which we can use for other applications such as treating cancerous tumours and treating bacteria and fungi. It damages normal cells and can potentially be employed as carriers for medications and other purposes.

#### 5. ACKNOWLEDGEMENTS

The authors gratefully acknowledge support from University of Baghdad (College of Science for Women), Al-Yarmouk Hospital, Baghdad and University of Anbar (College of Science).

## 6. REFERENCES

1. Ghufran, S. J., Khawla, S. K. & Maha, J. A. (2021). Study the antibacterial activity of zinc oxide nanoparticles synthesis by laser ablation in liquid. *Mater. Today Proc.*, 42(5), 2668–2673. <https://doi.org/10.1016/j.matpr.2020.12.646>
2. Ashwini, J. et al. (2021). Synthesis and characterization of zinc oxide nanoparticles using *Acacia caesia* bark extract and its photocatalytic and antimicrobial activities. *Catalysts*, 11(12), 1507. <https://doi.org/10.3390/catal11121507>
3. Hasnidawani, J. N. et al. (2016). Synthesis of ZnO nanostructures using sol-gel method. *Proc. Chem.*, 19, 211–216. <https://doi.org/10.1016/j.proche.2016.03.095>
4. Faisal, S. et al. (2021). Green synthesis of zinc oxide (ZnO) nanoparticles using aqueous fruit extracts of *Myristica fragrans*: Their characterizations and biological and environmental applications. *ACS Omega*, 6(14), 9709–9722. <https://doi.org/10.1021/acsomega.1c00310>
5. Abbas, N. K., Shanan, Z. J. & Mohammed, T. H. (2022). Physical properties of Cu doped ZnO nanocrystalline thin films. *Baghdad Sci. J.*, 19(1), 0217. <https://doi.org/10.21123/bsj.2022.19.1.0217>
6. Shaker, D. S., Abass, N. K. & Ulwall, R. A. (2022). Preparation and study of the structural, morphological and optical properties of pure tin oxide nanoparticle doped with Cu. *Baghdad Sci. J.*, 19(3), 0660. <https://doi.org/10.21123/bsj.2022.19.3.0660>
7. Ayman, E. et al. (2023). An overview of the public health challenges in diagnosing and controlling human foodborne pathogens. *Vaccines*, 11(4), 725. <https://doi.org/10.3390/vaccines11040725>
8. Siddiqi, K. S. & Husen, A. (2018). Properties of zinc oxide nanoparticles and their activity against microbes. *Nanoscale Res. Lett.*, 13(1), 1–13. <https://doi.org/10.1186/s11671-018-2532-3>
9. Mehrabian, M. et al. (2011). UV detecting properties of hydrothermal synthesized ZnO nanorods. *Physica E Low Dimens. Syst. Nanostruct.*, 43(6), 1141–1145. <https://doi.org/10.1016/j.physe.2011.01.030>
10. Ali, S. M. U. et al. (2010). A fast and sensitive potentiometric glucose microsensor based on glucose oxidase coated ZnO nanowires grown on a thin silver wire. *Sens. Actuators B Chem.*, 145(2), 869–874. <https://doi.org/10.1016/j.snb.2009.12.072>
11. Kashif, M. et al. (2012). Morphological, optical, and Raman characteristics of ZnO nanoflakes prepared via a sol–gel method. *Phys. Status Solidi A-Appl. Mat.*, 209(1), 143–147. <https://doi.org/10.1002/pssa.201127357>
12. Mohammed, A. M. et al. (2017). Nanostructured ZnO-based biosensor: DNA immobilization and hybridization. *Sens. Bio-Sens. Res.*, 15, 46–52. <https://doi.org/10.1016/j.sbsr.2017.07.003>
13. Ansari, M. T. et al. (2018). Applications of zinc nanoparticles in medical and healthcare fields. *Curr Nanomed*, 8(3), 225–233. <https://doi.org/10.2174/2405461503666180709100110>
14. Zhang, Z. Y. & Xiong, H. M. (2015). Photoluminescent ZnO nanoparticles and their biological applications. *Materials*, 8(6), 3101–3127. <https://doi.org/10.3390/ma8063101>

15. Kim, S., Lee, S. Y. & Cho, H. J. (2017). Doxorubicin-wrapped zinc oxide nanoclusters for the therapy of colorectal adenocarcinoma. *Nanomater.*, 7(11), 354. <https://doi.org/10.3390/nano7110354>
16. Adil, B. H., Aadim, K. A. & Khalaf, M. A. (2021). Synthesis and spectroscopic characterization of platinum nanoparticles by plasma jet method. *Int. J. Nanosci.*, 20(03), 2150030. <https://doi.org/10.1142/S0219581X21500307>
17. Kaith, W. K. et al. (2022). Effect of cold atmospheric plasma on osteoporosis by FE-DBD system. *Plasma Med.*, 12(3), 69–80. <https://doi.org/10.1615/PlasmaMed.2022046356>
18. Adil, B. H. et al. (2021). Effect of cold plasma on the levels mineral blood components in vivo. *Key Eng. Mater.*, 886, 177–182. <https://doi.org/10.4028/www.scientific.net/KEM.886.177>
19. Obaid, A. S., Mahdi, M. A. & Hassan, Z. (2012). Nanocoral PbS thin film growth by solid-vapor deposition. *Optoelectronics Adv. Mater. – Rapid Commun.*, 6(3–4), 422–426.
20. Raka, J. M. & Obaid, A. S. (2020). Preparation of nanoparticles in an eco- friendly method using thyme leaf extracts. *Baghdad Sci. J.*, 17(2), 670–674. [https://doi.org/10.21123/bsj.2020.17.2\(SI\).0670](https://doi.org/10.21123/bsj.2020.17.2(SI).0670)